Evidence for Protein Dielectric Relaxations in Reaction Centers Associated with the Primary Charge Separation Detected from *Rhodospirillum rubrum* Chromatophores by Combined Photovoltage and Absorption Measurements in the 1−15 ns Time Range[†]

Hans-Wilhelm Trissl,* Karen Bernhardt, and Mikhail Lapin

Abteilung Biophysik, University of Osnabrück, Fachbereich Biologie/Chemie, Barbarastrasse 11, D-49069 Osnabrück, Germany

Received August 10, 2000; Revised Manuscript Received January 23, 2001

ABSTRACT: Fast photovoltage measurements in *Rhodospirillum rubrum* chromatophores in the nanosecond time range, escorted by time-resolved absorption measurements, are described. Under reducing conditions, the photovoltage decayed significantly faster than the spectroscopically detected charge recombination of the radical pair $P^+H_A^-$. This indicates the occurrence of considerable dielectric relaxations. Our data and data from the literature were analyzed by means of a reaction scheme consisting of three states, namely, A*, P*, and $P^+H_A^-$. A time-dependent $\Delta G(t)$ was introduced by assuming a time-dependent rate constant of the back-reaction, $k_{-1}(t)$. With the exception of the latter rate constant, all other parameters of the model are reliably known within narrow limits. This allowed us to distinguish between the three cases assumed for $\Delta G°(t)$: ${}^1\Delta G°(t) =$ constant; ${}^2\Delta G°(t)$ as published by Peloquin et al. [Peloquin, J. M., Williams, J. C., Lin, X. M., Alden, R. G., Taguchi, A. K. W., Allen, J. P., and Woodbury, N. W. (1994) *Biochemistry 33,* 8089−8100]; and a ${}^3\Delta G°(t)$ that fits the present data. The assumption that ${}^1\Delta G°(t) =$ constant is incompatible with our photovoltage data, and ${}^2\Delta G°(t)$ is incompatible with the constraint that the ratio of fluorescence yields in the closed and open state is $F_m/F_o \approx 2$. We specify a ${}^3\Delta G°(t)$ that should be valid for photosynthetic reaction centers in vivo. Furthermore, the overall kinetics of the electric relaxation, $e(t)$, in response to the primary charge separation were determined.

The three-dimensional representation of the bacterial reaction center that has emerged from X-ray crystallographic analysis suggests a rigid and immobile structure. However, proteins are known to fluctuate substantially around an average structure (*1*). At room temperature, proteins can assume many nearly isoenergetic conformational substates separated by energy barriers varying widely in height. Accordingly, transitions between the substates occur on time scales spread over many orders of magnitude.

With decreasing temperature, protein fluctuations become frozen (*2*). In this case, a macroscopic sample consists of a heterogeneous ensemble of structurally different substates. At ambient temperature, however, protein conformational dynamics may dictate the enzymatic reaction rate and also be responsible for a distribution of rate constants. If the fluctuations between the substates are faster than the molecular reaction, kinetics may be nonexponential due to protein dynamics. However, kinetic averaging may lead to apparently single-valued rate constants (*3*). If the fluctuations are slower than the molecular reaction, kinetics become nonexponential due to the inherent disorder of proteins (*2, 4, 5*).

In bacterial reaction centers, dielectric protein relaxations are thought to play a central role in the primary photosynthetic charge separation and the subsequent stabilization reactions [for review, see (*6*)]. Multiphasic kinetics have been observed for charge recombination reactions of the primary charge-separated state ($P^+H_A^- \rightarrow PH_A$) as well as for the charge-stabilized state ($P^+Q_A^- \rightarrow PQ_A$). These two back-reactions occur on very different time scales: $P^+Q_A^-$ recombines with a time constant of approximately 100 ms whereas $P^+H_A^-$ has a decay time of approximately 10 ns. In most publications, the multiexponential behavior of the charge recombination luminescence in isolated RCs (*7*) is explained by a static distribution of conformational states (*8*−*10*). The multiphasicity of the $P^+H_A^- \rightarrow P^*H_A \rightarrow h\nu$ reaction, observed at all temperatures, was also explained by a dynamic solvation process in a homogeneous ensemble of RCs (*11*−*13*), giving rise to a description of the protein relaxations connected with the solvation of P^+ and H_A^- by a time-dependent free energy change, $\Delta G°(t)$. However, consideration of dispersive kinetics of the forward charge separation that extends up to 1 ns (*14, 15*) might necessitate a reevaluation of Peloquin's work (*13*).

Other direct evidence for relaxations in response to the charge separation in RCs comes from photoacoustic measurements, which indicate a volume contraction (electrostriction) within 50 ns in RCs (*16*). Electrostriction in RCs had been observed earlier though with lower time resolution (*17, 18*).

Another experimental assay to demonstrate the existence of conformational changes involves trapping of substates at

[†] The work was financially supported by the Deutsche Forschungsgemeinschaft (SFB 171, TP A1, and TR 129/7-1).

* Address correspondence to this author. E-mail: trissl@uos.de.

10.1021/bi001885u CCC: $20.00
Published on Web 04/06/2001

low temperature. In this case, flash spectroscopic measurements display different multiexponential kinetics depending on preillumination and freezing conditions (*3, 19*−*23*).

In the present work, we used a combination of spectroscopic and photoelectric measurements to show that during the lifetime of the $P^+H_A^-$ radical pair state significant dielectric protein relaxations occur.

The most relevant experimental evidence for a dynamic solvation has been gained from the multiphasic fluorescence decay kinetics of isolated purple bacteria RCs, solubilized by detergents (*11*−*13*). These, however, may behave unlike those in vivo, as noted in (*24 , 25*) where the recombination kinetics in chromatophores and isolated RCs are found to be significantly different. Differences between chromatophores and RCs were also observed in the formation kinetics of the primary charge separation (*26*).

The question whether the same or a different $\Delta G°(t)$ to the one published by Peloquin et al. (*13*) for detergent-isolated RCs is as valid in situ as in the chromatophore membrane has not been considered so far. It is therefore worth studying such an intact system. We have selected the chromatophores from *Rhodospirillum* (*Rs.*) *rubrum* for our study, because this species is known to possess a totally invariable antenna system and allows for highly reproducible preparations.

If the RC is surrounded by antenna pigments (A), the prompt fluorescence (F_o), which is due to the trapping process, as well as the recombination luminescence (F_v) is emitted predominantly by A* whereas emission by P* is negligible (*27*). As is shown here by a model calculation, any multiphasic recombination kinetics in the RC lead to corresponding multiphasic excited state kinetics in the antenna. These phases are as equally well apparent as in isolated RCs. The main difference between the two systems is a restricted time resolution of the intact system since, during the trapping process (≈70 ps), the yield of the prompt fluorescence exceeds by far the fluorescence yield due to charge recombination.

By a combined analysis of flash-induced absorption and fast photovoltage measurements with chromatophores under reducing conditions, we have shown that the photovoltage decayed markedly faster than the spectroscopically detected radical pair recombination. This demonstrates unambiguously the existence of significant protein relaxations in the RC moiety associated with the solvation of the primary radical pair.

MATERIALS AND METHODS

Chromatophore Preparation. Rs. rubrum cells were cultured according to (*28*) and chromatophores prepared according to (*29*). The chromatophores were suspended in 10 mM TRIS, pH 7.4, with 25% (v/v) glycerol and stored at −80 °C until use.

Absorption Kinetics. Time-resolved absorption measurements were performed in collaboration with Dr. K. Brettel (CEA Saclay) with the apparatus described prviously (*25*). Briefly, the sample was excited by 532 nm laser flashes of 300 ps duration. The measuring light was provided by a laser diode emitting at 970 nm, and the transmitted light was detected by a photodiode (model 3117; Lasermetrics). The signals were recorded with a digitizing 1 GHz oscilloscope (Tektronix DSA 602A). The apparatus transmission characteristics were obtained by scattered light from the laser. Absorption transients were fitted using exponential functions with offsets convoluted with the apparatus response function (Gaussian width of $\sigma = 0.70$ ns).

Photovoltage Measurements. Photovoltage measurements were performed in a 100 μm thick capacitative microcoaxial cell described previously (*30*). Nonsaturating excitation flashes at 532 nm with 30 ps duration were produced by a Nd:YAG laser. The excitation energy corresponded to ≈1 hit per PSU. The photovoltage signals were recorded at a repetition rate of 0.2 Hz with a 7 GHz digitizing oscilloscope (Tektronix 7250).

Photovoltage signals originated from irreversibly oriented layers of so-called purple membranes (isolated from *Halobacterium halobium*) or chromatophores, which were prepared in the cell through sedimentation of concentrated purple membranes/chromatophores by electric field pulses (several pulses of 10 V for 100 ms). These 10−30 μm thin gelatinous layers were then overlaid with the redox buffer. They remained stable for more than 30 min as judged by the constant amplitude of the photovoltage signals over that time range. Control experiments showed that the diffusion of the buffer into the layer required several minutes. The redox buffer (3 mM TRIS, 2 mM ascorbate, 1 mM TMPD, and 200 μM terbutryn, pH 7.6) was optimized for keeping all RCs open in the dark and a high fraction of RCs reduced in the light.

Typically, photovoltage signals originating from a step-function charge separation decay biphasically (time constants of 1−2 and 20−1000 ns) based on a 50 Ω impedance of the recording electronics (*30*). The depicted photovoltage traces were disentangeled from the apparatus decay by deconvolution (*31*). Any remaining kinetics in these deconvoluted traces then indicate electrogenic processes occurring in the sample, i.e., e^--transfer reactions and dielectric relaxations.

All experiments were performed at room temperature (RT) of 20 ± 1 °C.

RESULTS

Model Calculations. In this section, we inspect the simple reaction schemes in Figure 1 with respect to fluorescence yields, fluorescence kinetics, and kinetics of the radical pair recombination and compare the simulated results for time-invariable and time-dependent rate constants. The figure compares kinetic schemes valid both for isolated RCs (a hypothetical case which assumes identical properties of RCs in the chomatophore membrane and in the detergent-solubilized state) and for photosynthetic units (PSU, 1 RC connected to 32 BChl *a* antenna pigments) in the chromatophore membrane. Rate constants that are dependent on the redox state of Q_A are labeled with superscripts 'o' and 'c'. All four reaction schemes were solved for excitation into P (RCs) or A (PSU) by matrix operations (*32*).

Numerical values for *Rs. rubrum*, assuming time-invariable rate constants, have been assessed recently [see (*27*) and references cited therein]. Most of these values (listed in Table 1) are experimentally well determined. Two of them, the rate constant for radiationless recombination of the radical pair into the ground state, k_d, and that for its recombination into the excited singlet state, k_{-1}, were redetermined in the present

Table 1: Reciprocal Rate Constants Taken from Reference (*27*) and Newly Determined in the Present Analysis (in Parentheses) under the Assumption of Time-Independent Rate Constants[a]

$1/k_t$	$1/k_{-t}$	$1/k_1^o$	$1/k_1^c$	$1/k_{-1}$	$1/k_d$	$1/k_2$	$1/k_l$	$\Sigma\chi^2$
69 ps	24 ps	2.4 ps	4.8 ps	900 ± 300 ps	5.7 ± 2 ns	220 ps	700 ps	29
				(1.2 ± 0.1 ns)	(7.9 ± 0.1 ns)			23

[a] The actual numbers for isolated RCs yield $F_m/F_o = 12.23$ and for the PSU $F_m/F_o = 2.27$. The apparent time constants (eigenvalues) that govern the radical pair decay kinetics are 7.6 ns for isolated RCs and 6.9 ns for PSUs.

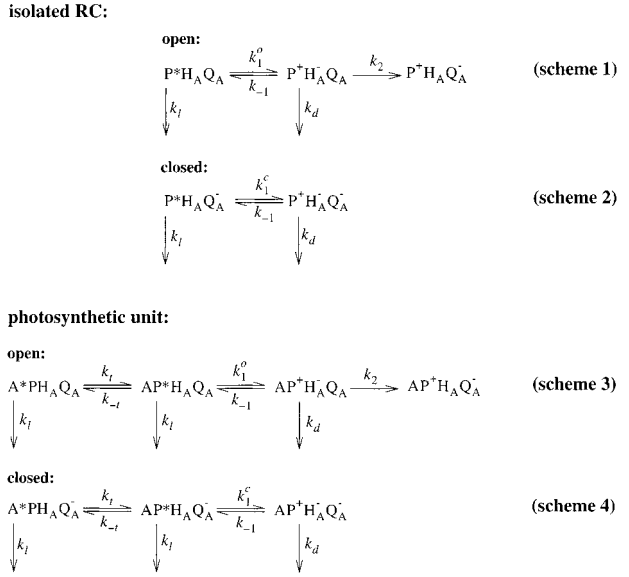

FIGURE 1: Ideal reaction schemes for hypothetically isolated RCs and photosynthetic units (RCs surrounded by antenna) for open and closed states. The molecular rate constants of the primary photochemistry are assumed to be identical in isolated RCs and in PSUs. The numerical values of the rate constants used are listed in Table 1.

work due to the availability of additional confining experimental data (absorption measurements; Figure 3b). The rate constant for radiationless losses of P* was set equal to the one in the antenna. Taking larger values, such as $(0.3\ \text{ns})^{-1}$ (*33*) for the latter, had no significant effect on the simulations.

In a first simulation with time-independent rate constants (Table 1), we investigated the extent to which the radiative processes in the RC are communicated to the antenna. It turned out that nanosecond phases of P*(t) due to the back-reaction can be observed also via emission from the antenna. This is in agreement with a high escape probability under reducing conditions (*27*). Therefore, the multiphasic fluorescence decay reported for isolated RCs (*13*) should also be detectable in chromatophores.

In a second simulation, also with time-independent rate constants, we inspected the influence of the presence or absence of antenna pigments on the radical pair decay kinetics by comparing the isolated RC with the photosynthetic unit. The numbers quoted in Table 1 yield time constants of 7.6 and 6.9 ns, respectively. Therefore, the widespread values for the charge recombination kinetics reported in the literature cannot be ascribed to the presence or absence of antenna pigments [see discussion in Gibasiewics et al. (*25*)].

In a third simulation, we investigated the consequences of time-dependent rate constants on the fluorescence yields and the radical pair recombination kinetics in PSUs. According to the fundamental relationship between the Gibbs energy and the rate constants [$\Delta G° = -RT \ln(k_1/k_{-1})$], any time-dependent $\Delta G°(t)$ of the primary charge separation can formally be ascribed to either one time-dependent rate constant (forward or backward) or both. Although for a given redox state the forward reaction could well be controlled by the dynamics of amino acid side groups (*34*), its value appears rather invariable with regard to experimental conditions. Therefore, we decided to perform our model calculations with a time-dependent rate constant for the charge recombination into the excited singlet state, $k_{-1}(t)$. For a given time course of $\Delta G°(t)$, this rate constant is calculated by

$$k_{-1}(t) = k_1 e^{\Delta G°(t)/RT} \quad (1)$$

We solved numerically the systems of differential equations belonging to the schemes of Figure 1 for three different $\Delta G°(t)$: (i) ${}^1\Delta G°(t) = -131$ meV (*27*), (ii) ${}^2\Delta G°(t)$ taken from Peloquin et al. (*13*), and (iii) ${}^3\Delta G°(t)$ which is consistent with all experimental constraints. To describe the time dependence, we used an exponential function:

$$\Delta G°(t) = \Delta G°(\infty) + \left(\sum_{i=1}^{4} a_i e^{-t/\tau_i}\right)[\Delta G°(0) - \Delta G°(\infty)] \quad (2)$$

The time courses chosen are depicted in Figure 2a, and the parameters are given in the figure legend.

The model calculations for PSUs show that the case of a constant ${}^1\Delta G°(t)$ fulfills the $F_m/F_o \approx 2$ criterion but, due to the absence of relaxations, it does not predict multiphasic fluorescence decay kinetics. Vice versa, the time course of ${}^2\Delta G°(t)$ published by Peloquin et al. (*3*) does predict multiphasic fluorescence decay kinetics but leads to a rather small F_m/F_o of 1.1−1.2. Hence, it does not fulfill the $F_m/F_o \approx 2$ criterion. Only the third case, ${}^3\Delta G°(t)$, fulfills both criteria.

Figure 2b shows the simulated fluorescence decay in PSUs for all three cases above. The most pronounced differences occur in the 0.5−15 ns time interval, where also the multiple phases arising from time-dependent $\Delta G°(t)$ are clearly recognizable by comparison with the purely biphasic decay (apparent time constants of 74 ps and 6.9 ns) valid for ${}^1\Delta G°(t) = \text{constant}$.

Furthermore, for all three cases, we calculated the time courses of the transiently formed radical pair in PSUs (Figure 2c). It turned out that the different assumptions of $\Delta G°(t)$ led to nearly indistinguishable traces. In particular, the decaying part is essentially monophasic, with a time constant close to $1/k_d$ (rate constants for defining $\Delta G°$ are given in the legend of Figure 2).

Differences in the kinetics due to the three model assumptions are rather obvious in the fluorescence (Figure 2b) but appear insignificant in the absorption measurements (Figure

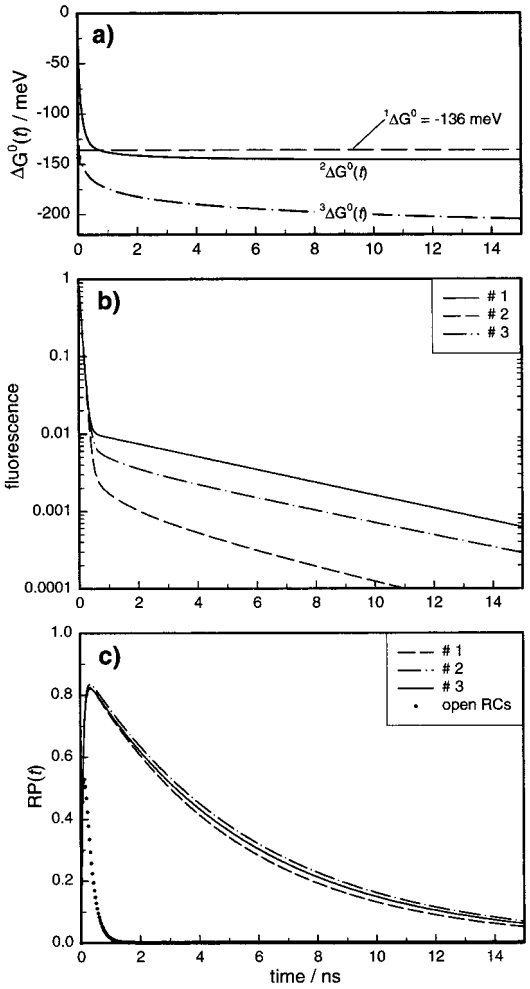

FIGURE 2: (a) Three time courses of the Gibbs energy $\Delta G(t)$ assumed for the model calculations. Parameters for $^2\Delta G°(t)$: a_i = 0.8/0.1/0.1/0.15, τ_i = 0.01/0.2/1/8.5 ns, $^2\Delta G°(0)$ = 0 meV, and $^2\Delta G°(\infty)$ = −210 meV. Parameters for $^3\Delta G°(t)$: a_i = 0.34/0.55/0.07/0.04, τ_i = 0.01/0.1/0.9/4 ns, $^3\Delta G°(0)$ = 0 meV, and $^3\Delta G°(\infty)$ = −146 meV. (b) Simulated fluorescence decay in PSUs under reducing conditions due to the three different assumptions of $\Delta G°(t)$. (c) Simulated time course of the radical pair transients in PSUs under reducing conditions due to the three different assumptions of $\Delta G°(t)$.

2c), even though for both assays the same molecular rate constants are used. This fact explains why phases that are well resolved in fluorescence decay measurements are not necessarily found in absorption measurements (*35*−*37*).

Absorption Measurements. Flash-spectroscopic absorption difference measurements under reducing conditions were performed with *Rs. rubrum* chromatophores suspended in 10 mM TRIS (pH 7.8) and 10 mM dithionite. The kinetics of the absorption change at 970 nm are shown in Figure 3. Decay of the radical pair after trapping is complete (ca. 100 ps) was fitted by a single-exponential function with τ_{opt} = 6.9 ns according to:

$$c_{rp}(t) = e^{-t/\tau_{opt}} \quad (3)$$

The choice of two or more exponential functions did not improve the fit. Other experimental protocols (chemical reduction with different dithionite concentrations and reduction by background light without dithionite) yielded, within statistical fluctuations between repeated experiments, time

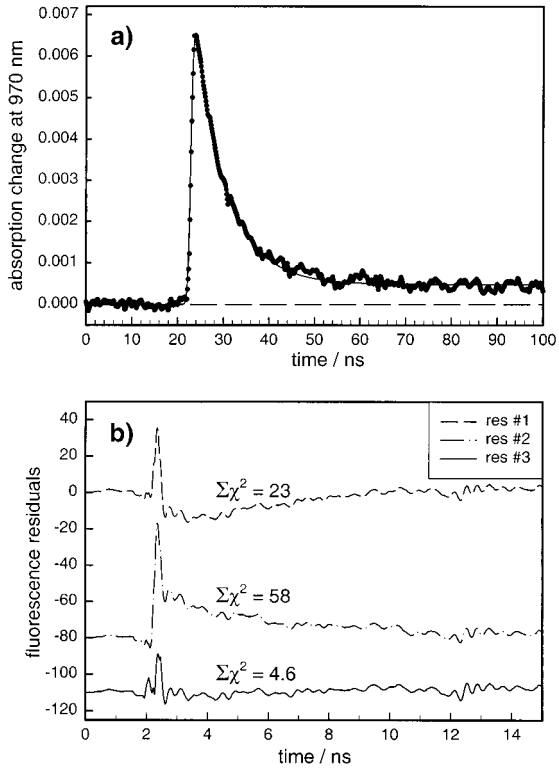

FIGURE 3: (a) Absorption change at 970 nm measured in *Rs. rubrum* chromatophores under reducing conditions (data points). Fit of the data (solid line) as described in the text. (b) Reanalysis of the fluorescence decay published in (*27*). Residuals for the cases of three different $\Delta G(t)$ shown in Figure 2a. The residuals are displaced arbitrarily.

constants in the range of 6.7−7.1 ns. Although, in the framework of a continuous relaxation of the primary radical pair, the kinetics are expected to be multiphasic (Figure 2c; solid and dash−dot lines), such deviations from the monoexponential description could not be resolved. However, other authors have noticed a slight kinetic inhomogeneity in transient absorption measurements (*38*).

Fluorescence Measurements. Time-resolved fluorescence measurements with *Rs. rubrum* chromatophores under reducing conditions (5 mM dithionite, 5 mM TRIS at pH 7.8) have been published by us recently (*27*). The aim in this work was to find the conceptually most simple three-state model that describes the basic features of trapping and detrapping in photosynthetic units of purple bacteria. However, details such as possible sample heterogeneities, dispersive kinetics, and time-dependent rate constants were not considered. Consequently, the global fits in (*27*) do not represent unimprovable 'best fits' of single experiments, such as time-resolved fluorescence decays. Specifically, the rate constants k_{-1} and k_d could not be assessed with high accuracy because they tend to compensate each other.

Here we reanalyze the particular fluorescence transient shown in (*27*), using the three different $\Delta G°(t)$ functions (Figure 2a). The best fit of each $\Delta G°(t)$ provided us with the parameters for $^1\Delta G$ and $^3\Delta G(t)$ listed in the legend of Figure 2.

In the case of constant $^1\Delta G$, the residuals (Figure 3b, upper trace) display significant positive and negative lobes yielding $\Sigma\chi^2$ = 23. For the fit, we used the constraint that the time constant of the radical pair decay (as determined from the

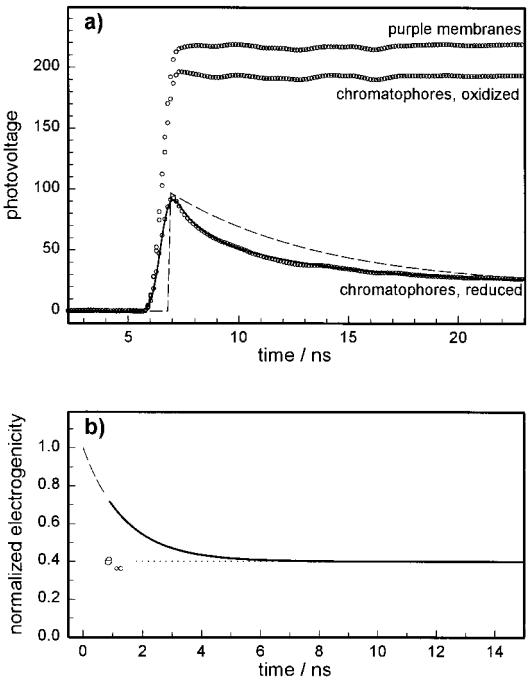

FIGURE 4: (a) Deconvoluted photovoltage traces from purple membranes (upper trace) and from oxidized and reduced chromatophores (lower traces; points) subjected to the redox buffer defined in the text. Two theoretical curves were adjusted to the data for reduced chromatophore decay. One (dashed line) was adjusted to the initial maximum and the asymptote value having the same kinetics as the absorption change (Figure 3). The other one (solid line) also takes dielectric relaxations into account and fits the experimental curve. (b) Time course of the normalized dielectric relaxation $[e_{rp}(t)/e_0]$ of the radical pair (used for the above fit) according to eq 4 with the parameters $\tau^{el} = 1.4$ ns, and $e_\infty = 0.4$.

absorption measurement) was 6.9 ns. This resulted in values for k_{-1} and k_d that deviate from those in (*27*). Table 1 summarizes the numerical values used. The small difference between the $\Sigma\chi^2$ belonging to the two sets of rate constants illustrates the compensatory effect mentioned (Table 1, last column).

In the case of Peloquin et al.'s $^2\Delta G(t)$, the residuals (Figure 3b, middle trace) show only strong positive deviations and a $\Sigma\chi^2 = 58$. In contrast, the case of $^3\Delta G(t)$ yields rather small residuals (Figure 3b, lower trace) with $\Sigma\chi^2 = 4.6$.

Photovoltage Measurements: Control Experiments. To determine the parameters that are valid for the apparatus decay function, we recorded the photovoltages from oriented purple membranes and chromatophores, both immersed in an identical redox buffer (Materials and Methods) intended to keep the RCs in the chromatophore layer open in the dark (Figure 4). The same electrolyte conditions should guarantee the same decay parameters in both experiments. Figure 4 shows that in both cases the deconvolution of both traces (uppermost curves) with the same decay function yields rather clean step functions.

In the time range covered in our experiments, only the K-intermediate of the bacteriorhodopsin photocycle persists (*39*−*41*). Assuming the bacteriorhodopsin protein does not undergo conformational changes in this time domain (*42*−*44*), it can be concluded that RC relaxations connected with the full charge separation $P^* \rightarrow P^+Q_A^-$ are small and close to the detectable limit of our assay.

Photovoltages from Oriented Chromatophore Layers under Reducing Conditions. To avoid obscuration of possible dielectric relaxations in the protein by the apparatus decay function, the photovoltage experiments were designed so that both data sets for open and closed RCs could be obtained from a single chromatophore layer immersed in one and the same redox buffer (see Materials and Methods). These invariable conditions justified performing the data analysis with the same apparatus decay function. The transition from the open to the closed state was initiated by background illumination. To obtain a large fraction of RCs with Q_A^- at moderate background light intensities, terbutryn was used to block the electron transfer from Q_A to Q_B. However, the background light exposure might create a mixture of the active states PH_AQ_A, $PH_AQ_A^-$, and the inactive oxidized state $P^+H_AQ_A^{(-)}$, with the relative fractions depending on both the exact redox buffer composition and the light intensity. These fractions can be estimated from their typical shape in photovoltage experiments: PH_AQ_A produces a fast rising step function, whereas $PH_AQ_A^-$ produces a fast rising transient decaying with approximately 7 ns due to charge recombination of $P^+H_A^-$. The third fraction of inactive RCs, possessing the oxidized primary donor P^+, produces no signal but its concentration can be deduced from analysis of the initial amplitudes, as explained in detail below.

Figure 4a shows the deconvoluted photovoltages of a chromatophore layer under the above conditions with and without background illumination. The dark-adapted trace displays a nearly rectangular shape whereas the trace obtained with background light displays a decay close to the baseline. In the first approximation, this decaying part can be ascribed to charge recombination of the radical pair in reduced RCs. Approximately 100 ms after the last background light exposure, the photovoltage signals were indistinguishable from those recorded initially in the dark-adapted state. Background light of various intensities yielded qualitatively similar results, but the initial and final amplitudes differed.

At the first stage of analysis, we investigated whether the photovoltage decay originating from the background-illuminated layers matched the kinetics of the absorption transient. For this purpose, we attempted to adjust a single-exponential decay function (with the time constant of 6.9 ns) to the photovoltage data (Figure 4a; dashed curves). A deviation of this mathematical curve from the data points is clearly noticeable. The photovoltage decay was also faster than the absorption transient in experiments that utilized different chromatophore layers and various redox buffers. Therefore, it seems safe to conclude that the accelerated photovoltage decay indicates an electrogenic reaction that is spectroscopically invisible but is well apparent in photovoltage measurements.

Assuming the decay due to the apparatus response is the same, the step-function appearance of the deconvoluted traces of purple membranes and dark-adapted chromatophores (Figure 4a, top traces) suggests that the dark-adapted chromatophores contain only open RCs. If the corresponding maximal photovoltage amplitude is labeled A_0^{da} (Figure 5), then the initial photovoltage amplitude with background light, A_0^{la}, is the sum of the photovoltages from the fraction of still open RCs, $A_{op} = f_{op} \cdot A_0^{da}$, and the fraction of reduced RCs, f_{red} [weighted with the initial relative electrogenicity, e_0, of the radical pair $P^+H_A^-$: $A_{red} = f_{red} \cdot e_0 \cdot A_0^{da}$ (Figure 5)].

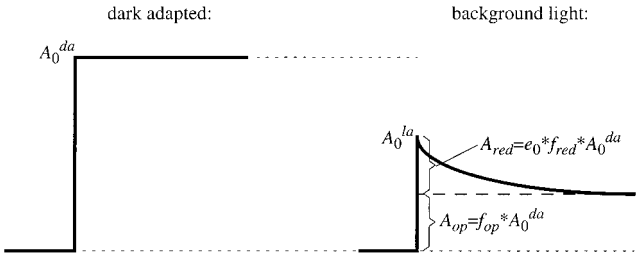

FIGURE 5: Schematic presentation of the photovoltages induced by the primary charge separation for the cases of the oxidized (left) and reduced (right) acceptor site of RCs.

The fraction of the oxidized state $P^+H_AQ_A^{(-)}$, f_{ox}, produces no contribution to the photovoltage signal, but the condition $f_{op} + f_{red} + f_{ox} = 1$ must be fulfilled.

We approximated protein dielectric relaxation by an exponential function (the time constant τ^{el}) which converges to e_∞ for infinite times:

$$e_{rp}(t) = e_0 \cdot \left\{ \exp\left(-\frac{t}{\tau^{el}}\right) \cdot (1 - e_\infty) + e_\infty \right\} \qquad (4)$$

The initial amplitude e_0 represents the electrogenicity of the unrelaxed radical pair, which is expected to be $e_0 \approx 0.45$ from structural data (*45*). It is normalized to the full charge separation $P^+H_AQ_A^-$, whose amplitude was set to 1.

The function (eq 4) is illustrated in Figure 4b with the parameters listed in the legend. According to the above definitions, the time course of the electric response in the light-adapted case is

$$e(t) = f_{op} \cdot A_0^{da} + f_{red} \cdot A_0^{da} \cdot c_{rp}(t) \cdot e_{rp}(t) \qquad (5)$$

To fit an experimental light-adapted trace, this function was convoluted with the apparatus response function $G(t)$, which was assumed to be a Gaussian:

$$pv(t) = e(t) \otimes G(t) \qquad (6)$$

The Gaussian width (470 ps) was obtained from the rising part of the dark-adapted signal.

Best fits to the data (Figure 4, solid curves) collected with different background light intensities were obtained with $e_0 = 0.54$, $e_\infty = 0.4$, and $\tau^{el} = 1.4$ ns. These numerical values could be determined with different accuracy. For instance, e_0 could not be chosen to be <0.5 because the initial photovoltage amplitude under reducing conditions is high even if RCs with P^+ are assumed to be absent. The parameter e_∞ is then determined with an accuracy of $\pm 15\%$. When e_0 and e_∞ are set, the time constant τ^{el} follows with approximately 10% accuracy. However, since e_∞ and the time constant can compensate each other to some extent, the error of these three parameters is estimated to be $\pm 20\%$.

DISCUSSION

Sample Heterogeneity. The interpretation of nonexponential kinetics is not trivial. Several factors may be responsible for nonhomogeneous samples and the resulting multiphasic kinetics. First we will discuss a possible macroscopic heterogeneity of the sample which can be due to the isolation procedure giving rise to distinct long-lived (i.e., static) conformational states of the RCs. Detergent-isolated RCs may be more susceptible to static heterogeneities than chromatophore preparations. Consequently, Peloquin et al. (*13*) had to argue thoroughly that their RC preparation did not contain distinct populations. However, definite proof is not possible in view of many reports in which distinct conformations of the RC depending on pH, redox potential, and illumination have been identified (*19*, *23*, *46*, *47*).

In the case of our *Rs. rubrum* chromatophores, it could be argued that the sample is likely to be homogeneous since this bacterium possesses a particularly invariable antenna system (fixed stoichiometric ratio of antenna pigments to RC) that allows for highly reproducible preparations. Nonetheless, the presence of RC substate populations in chromatophores cannot be excluded, since any e^--transfer reaction that is faster than the time scale of conformational changes will occur in a heterogeneous ensemble of proteins with a distribution of transition states (*3*). This consideration points out the need for an electrical assay, like the photovoltage technique, that is capable of probing protein relaxations directly.

Distribution of Conformational Substates versus Dynamic Relaxation during the Lifetime of the Radical Pair. There is a fundamental difference between the two explanations for the occurrence of multiphasic fluorescence decay kinetics in reduced RCs. In the framework of dynamic relaxation or time-dependent thermodynamics, protein conformational dynamics in the nanosecond range are the cause for nonexponential kinetics, whereas in the framework of conformational substates each substate is static on the time scale of the reaction. Although the charge separation for each substate may be exponential, the sum over all existing substates then causes nonexponential kinetics. Accordingly, the former explanation predicts a dielectric protein relaxation in the nanosecond range whereas the latter explanation does not. An appropriate assay to experimentally determine such dielectric relaxations is the fast photovoltage technique that has been used in this study to distinguish between the two scenarios.

Our data on *Rs. rubrum* chromatophores display different kinetics of the primary radical pair decay whether detected spectroscopically or photoelectrically. Whereas absorption changes probe the time-dependent concentration of a state, photovoltage measurements probe the electrogenicity of the state. If the latter is time-dependent within the lifetime of the state, absorption change and photovoltage kinetics diverge. Since this has been demonstrated here (Figure 4a), we conclude that protein dielectric relaxations are intimately connected with the primary charge separation. In the time range covered by our measurements, they are surprisingly large (as shown in Figure 4b).

Similar experiments with *Rps. viridis* membranes have been published before (*25*). Different time courses of the spectroscopic and photovoltage signals have also been detected in this species (3.0 ± 0.2 ns versus 2.4 ± 0.2 ns, respectively). The authors suggested limitations of the methods were the cause for this discrepancy. However, in light of our present results, the divergence observed in *Rps. viridis* should also be considered as evidence of protein relaxations.

Dynamic Solvation versus Relaxed Radical Pair States. Like Peloquin et al. (*13*), we have used a time-dependent $\Delta G°(t)$ [via the time-dependent rate constant $k_{-1}(t)$; eq 1] to analyze our data. Alternatively, one could use the approach

of introducing several relaxed radical pair states that are formed in successive order and differ in their $\Delta G°$. We have also applied this latter approach to our data and obtained comparable fit qualities with two states. However, many combinations of their $\Delta G°$ and the rate constant with which the second state is formed are possible. Hence, this system is less satisfactorily defined than the present treatment and could not account for the continuity of the solvation process expected from the contribution of a large number of amino acid side groups.

The description of dynamic solvation by means of relaxed radical pairs is commonly applied to the RC of PS II (*48, 49*). This approach was also applied to theoretical calculations of the electrostatic control of primary charge separation in the bacterial RC (*50*). These calculations yielded an estimate of $\Delta G° = -87$ meV for the unrelaxed radical pair (referring to the static X-ray crytallographic structure) and of $\Delta G° = -304$ meV for the relaxed state. Whereas the former value represents an intermediate value within the early fast $\Delta G°(t)$ decay (Figure 2a), the latter one lies much lower than our value of -146 meV achieved after 15 ns. We believe that our convergence value of $^3\Delta G°(\infty) = -146$ meV represents the most reliable estimate for this particular time range.

Peloquin et al.'s $^2\Delta G(t)$ in Relation to Fluorescence Yield. If the time dependence of $\Delta G°(t)$ for isolated RCs published by Peloquin et al. (*13*) was the same as for RCs surrounded by light harvesting complexes embedded in the photosynthetic membrane, the predicted F_m/F_o in chromatophores would be much smaller than experimentally observed (section 3.1). We conclude that this particular $^2\Delta G°(t)$ is incompatible with the current experimental data. A closer inspection shows that this small F_m/F_o is due to the fast decrease of $^2\Delta G°(t)$ to rather large negative values (Figure 2a). The essential difference to the $^3\Delta G°(t)$ we suggest is the slower descent to less negative values that leads to more recombination luminescence.

A possible origin of this difference could be the presence of detergent molecules within the isolated RC that loosen up the structure and make the protein more fluid. The increased flexibility of the protein moiety may lead to a faster and more pronounced solvation of the radical pair in isolated RCs than in membrane-embedded RCs. Another reason for the incompatibility of Peloquin's $^2\Delta G°(t)$ with the F_m/F_o criterion could be the neglect of dispersive charge separation kinetics (*14, 15*) in reference (*13*).

Our $^3\Delta G(t)$. The rate constant of nonphotochemical losses of P*, k_l(P*), has been assumed here to be equal to the antenna losses, k_l(A*), namely, $(700\ \text{ps})^{-1}$. For hypothetical isolated RCs, this leads to $F_m/F_o = 12$ (Figure 1 legend). Measurements on experimental RC preparations, however, show $F_m/F_o = 3$ (*51*). This discrepancy may have two origins. First, k_l(P*) can be larger than assumed. To achieve the experimental F_m/F_o ratio, losses of P* should be equal to $k_l(P*) = (8\ \text{ps})^{-1}$ if all other parameters are kept the same. Second, the molecular rate constants of hypothetical isolated RCs may not apply to real isolated RCs because they may have other molecular properties. In this case, F_m/F_o can be easily tuned to 3 by changing k_{-1} and k_d appropriately. Then, however, as our model calculations show, F_m/F_o for the PSU would drop to 1.2, a value that does not agree with the experimental data.

As such, it can be concluded that detergent preparations of RCs display significantly different properties than in situ RCs. The incorporation of a few detergent molecules may lead to a softening of the packing density (*52*), a better solvation, and consequently a lower $\Delta G°$ at any given time.

Electric Relaxations Connected with Charge Separation. With open RCs, the deconvoluted photovoltage from chromatophore layers displayed an overall rectangular-shaped step-function with little indication of a relaxation up to 20 ns. This can be concluded from the very similar signal shapes for *Rs. rubrum* chromatophores and PM layers under the same redox and ionic strength conditions (Figure 4a). If we assume that protein conformational changes in bacteriorhodopsin are small in this time domain (*42, 44*), then the same should also apply to bacterial RCs (Figure 4a). Photovoltage experiments with open RCs in the longer time range from 100 ns to 50 μs also do not indicate large protein dielectric relaxations, as the signals connected with the full charge separation—apart from small electrogenic e^--transfer reactions at the donor and acceptor sites—are virtually a step-function (*53*−*56*).

The deconvoluted photovoltage under reducing conditions decayed much faster than the spectroscopically detected kinetics of the radical pair (Figure 4a). This unequivocally proves that significant dielectric relaxations are taking place during the lifetime of the primary radical pair. In accordance with the interpretations in earlier work (*11*), these relaxations should be ascribed to protein solvation processes that continuously decrease the Gibbs energy of this state [Figure 2a; $^2\Delta G°(t)$ and $^3\Delta G°(t)$].

Molecular candidates that may contribute to the primary radical pair's relaxation are the two water molecules near H_A (*57*), specific amino acid residues (for instance Glu^{L104} which is hydrogen-bonded to H_A), and a collectively acting ensemble of amino acids. We believe that the relaxation of the two water molecules is fast and has terminated before the photovoltage has reached is maximum. In contrast to water, relaxations of amino acids in solution are much slower [from 300 ps to several nanoseconds according to (*58*)], and they are therefore the most likely candidates. We suggest that an ensemble of amino acid side chains is involved, although a detailed picture can only be obtained from an extended molecular dynamics calculation similar to the one performed by Parson et al. (*50*).

Dielectric relaxations of the protein in response to the charge separation ($P^+H_A^-$) may not be the only explanation for the fast decay of the photovoltage under reducing conditions. In addition to such relaxations, the attractive electrostatic force between P^+ and H_A^- could decrease the $P-H_A$ distance if the corresponding protein binding pockets are not perfectly rigid but have some elasticity. According to molecular dynamics calculations, this effect seems to be small (*59*), but it acts on the dipole axis and therefore may be rather efficient.

The data in Figure 4a (upper two traces) indicate that protein relaxations due to the full charge separation are surprisingly small in this time window. Two aspects must be considered in search of an explanation for the small size of the relaxations in open RCs compared to reduced ones. First, the contribution of dielectric relaxations connected with the primary radical pair $P^+H_A^-$ in open RCs (Figure 4b) is expected to be small because this state has a short lifetime

and because its maximal concentration is small (formation in 70 ps and decay in 220 ps; dotted curve in Figure 2c). Second, the hundreds of water molecules that surround, hemispherically, P and Q_A at the membrane/water interfaces (*57*) may cause a partial electrostatic shielding by their rapid reorientation in the strong monopole fields near P^+ and Q_A^-. This reorientation is likely to be much faster than our present time resolution [water in the aqueous phase relaxes within ≈9 ps (*58*)]. Hence, our photovoltage measurements probe the partially relaxed $P^+Q_A^-$ state.

An unexpected result of the photovoltage measurements under reducing conditions (Figure 4a) is the rather high initial electrogenicity $e_0 = 0.54$ of the radical pair ($P^+H_A^-$), because the crystallographic data show that the distance between P and H_A is approximately 0.45 of the distance between P and Q_A (*60*). Possibly the effective initial dielectric permittivity of the protein around P and H_A is smaller than around Q_A.

In summary, it seems that the formation of $P^+Q_A^-$ involves many polarizable groups moving quickly and rather isotropically. In the photovoltage assay, this leads to little electrogenic relaxation within the present time window (1−15 ns). In contrast, the formation of $P^+H_A^-$ seems to involve fewer polarizable groups moving more slowly and enforcing a conformational change occurring preferentially in the direction of the primary radical pair axis and hence in the direction of the membrane normal. In the photovoltage assay, this leads to a significant electrogenic relaxation. Irrespective of the precise molecular mechanisms involved, our photovoltage measurements demonstrated the relevance of protein conformational dynamics for stabilizing the primary radical pair in the nanosecond range. These dynamics lead to time-dependent rate constants and, as a consequence, to a time-dependent thermodynamic description of radical pair formation.

ACKNOWLEDGMENT

We are grateful to Dr. K. Brettel and Dr. W. Leibl (CEA Saclay) for performing the absorption measurements and helpful discussions. We thank Dr. C. Law for critical reading of the manuscript.

REFERENCES

1. Frauenfelder, H., Petsko, G. A., and Tsernoglou, D. (1979) *Nature 280*, 558−563.
2. Frauenfelder, H., Parak, F., and Young, R. D. (1988) *Annu. Rev. Biophys. Biophys. Chem. 17*, 451−479.
3. McMahon, B. H., Müller, J. D., Wraight, C. A., and Nienhaus, G. U. (1998) *Biophys. J. 74*, 2567−2587.
4. Austin, R. H., Beeson, K. W., Eisenstein, K. K., Frauenfelder, H., and Gunsalus, I. C. (1975) *Biochemistry 14*, 5355−5373.
5. Frauenfelder, H., and Wolynes, P. G. (1994) *Phys. Today* 58−64.
6. Rubin, A. B., Kononenko, A. A., Shaitan, K. V., Pashchenko, V. Z., and Riznichenko, G. Y. (1994) *Biophysics 39*, 173−195.
7. Sebban, P., and Barbet, J. C. (1984) *FEBS Lett. 165*, 107−110.
8. Du, M., Rosenthal, S. J., Xie, X. L., Dimagno, T. J., Schmidt, M., Hanson, D. K., Schiffer, M., Norris, J. R., and Fleming, G. R. (1992) *Proc. Natl. Acad. Sci. U.S.A. 89*, 8517−8521.
9. Müller, M. G., Griebenow, K., and Holzwarth, A. R. (1992) *Chem. Phys. Lett. 199*, 465−469.
10. Kirmaier, C., and Holten, D. (1990) *Proc. Natl. Acad. Sci. U.S.A. 87*, 3552−3556.
11. Woodbury, N. W., and Parson, W. W. (1984) *Biochim. Biophys. Acta 767*, 345−361.
12. Woodbury, N. W., Peloquin, J. M., Alden, R. G., Lin, X. M., Lin, S., Taguchi, A. K. W., Williams, J. C., and Allen, J. P. (1994) *Biochemistry 33*, 8101−8112.
13. Peloquin, J. M., Williams, J. C., Lin, X. M., Alden, R. G., Taguchi, A. K. W., Allen, J. P., and Woodbury, N. W. (1994) *Biochemistry 33*, 8089−8100.
14. Hartwich, G., Lossau, H., Michel-Beyerle, M. E., and Ogrodnik, A. (1998) *J. Phys. Chem. 102*, 3815−3820.
15. Ogrodnik, A., Hartwich, G., Lossau, H., and Michel-Beyerle, M. E. (1999) *Chem. Phys. 244*, 461−478.
16. Mauzerall, D. C., Gunner, M. R., and Zhang, J. W. (1995) *Biophys. J. 68*, 275−280.
17. Arata, H., and Parson, W. W. (1981) *Biochim. Biophys. Acta 636*, 70−81.
18. Malkin, S., Churio, M. S., Shochat, S., and Braslavsky, S. E. (1994) *J. Photochem. Photobiol. B 23*, 79−85.
19. Goushcha, A. O., Kharkyanen, V. N., and Holzwarth, A. R. (1997) *J. Phys. Chem. B 101*, 259−265.
20. Noks, P. P., Lukashev, E. P., Kononenko, A. A., Venediktov, P. S., and Rubin, A. B. (1977) *Mol. Biol. 11*, 835−842.
21. Müh, F., Williams, J. C., Allen, J. P., and Lubitz, W. (1998) *Biochemistry 37*, 13066−13074.
22. Tiede, D., Kellogg, E., and Breton, J. (1987) *Biochim. Biophys. Acta 892*, 294−302.
23. Kleinfeld, D., Okamura, M. Y., and Feher, G. (1984) *Biochemistry 23*, 5780−5786.
24. Gibasiewics, K., Brettel, K., Dobek, A., and Leibl, W. (1998) in *Photosynthesis: Mechanisms and Effects. Proceedings of the XIth International Congress on Photosynthesis* (Garab, G., Ed.) pp 841−844, Kluwer Academic Publishers, Dordrecht.
25. Gibasiewics, K., Brettel, K., Dobek, A., and Leibl, W. (2000) *Chem. Phys. Lett. 315*, 95−102.
26. Beekman, L. M. P., Visschers, R. W., Monshouwer, R., Heer-Dawson, M., Mattioli, T. A., McGlynn, P., Hunter, C. N., Robert, B., van Stokkum, I. H. M., van Grondelle, R., and Jones, M. R. (1995) *Biochemistry 34*, 14712−14721.
27. Bernhardt, K., and Trissl, H.-W. (2000) *Biochim. Biophys. Acta 1457*, 1−17.
28. Drews, G. (1983) *Mikrobiologisches Praktikum*, Springer-Verlag, Berlin and Heidelberg.
29. Otte, S. C. M., Kleinherenbrink, F. A. M., and Amesz, J. (1993) *Biochim. Biophys. Acta 1143*, 84−90.
30. Trissl, H.-W., and Wulf, K. (1995) *Biospectroscopy 1*, 71−82.
31. Wulf, K., and Trissl, H.-W. (1995) *Biospectroscopy 1*, 55−69.
32. Holzwarth, A. R. (1996) in *Biophysical Techniques in Photosynthesis* (Amesz, J., and Hoff, A. J., Eds.) pp 75−92, Kluwer Academic Press, Dordrecht, The Netherlands.
33. Eberl, U., Gilbert, M., Keupp, W., Langenbacher, T., Siegl, J., Sinning, I., Ogrodnik, A., Robles, S. J., Breton, J., Youvan, D. C., and Michel-Beyerle, M. E. (1992) in *The photosynthetic bacterial reaction center II—structure, spectroscopy and dynamics* (Breton, J., and Vermeglio, A., Eds.) pp 253−260, Plenum Press, New York.
34. Cherepanov, D. A., Krishtalik, L. I., and Mulkidjanian, A. (2000) personal communication.
35. van Stokkum, I. H. M., Beekman, L. M. P., Jones, M. R., van Brederode, M. E., and van Grondelle, R. (1997) *Biochemistry 36*, 11360−11368.
36. Holzwarth, A. R., and Müller, M. G. (1996) *Biochemistry 35*, 11820−11831.
37. Schenck, C. C., Blankenship, R. E., and Parson, W. W. (1982) *Biochim. Biophys. Acta 680*, 44−59.
38. Volk, M., Ogrodnik, A., and Michel-Beyerle, M. E. (1995) in *Anoxygenic Photosynthetic Bacteria* (Blankenship, R. E., Madigan, M. T., and Bauer, C. E., Eds.) pp 595−626, Kluwer Academic Publishers, Dordrecht.
39. Lanyi, J. K. (1992) *J. Bioenerg. Biomembr. 24*, 169−179.
40. Trissl, H.-W. (1990) *Photochem. Photobiol. 51*, 793−818.
41. Lanyi, J. K. (1999) *Int. Rev. Cytol. 187*, 161−202.

42. Diller, R., Iannone, M., Cowen, B. R., Maiti, S., Bogomolni, R. A., and Hochstrasser, R. M. (1992) *Biochemistry 31*, 5567−5572.
43. Gerwert, K. (1999) *Biol. Chem. 380*, 931−935.
44. Subramaniam, S., Lindahl, I., Bullough, P., Faruqi, A. R., Tittor, J., Oesterhelt, D., Brown, L., Lanyi, J., and Henderson, R. (1999) *J. Mol. Biol. 287*, 145−161.
45. Allen, J. P., Feher, G., Yeates, T. O., Rees, D. C., Deisenhofer, J., Michel, H., and Huber, R. (1986) *Proc. Natl. Acad. Sci. U.S.A. 83*, 8589−8593.
46. Kalman, L., and Maroti, P. (1997) *Biochemistry 36*, 15269−15276.
47. Stowell, M. H. B., Mcphillips, T. M., Rees, D. C., Soltis, S. M., Abresch, E., and Feher, G. (1997) *Science 276*, 812−816.
48. Roelofs, T. A., and Holzwarth, A. R. (1990) *Biophys. J. 57*, 1141−1153.
49. Schlodder, E., and Brettel, K. (1988) *Biochim. Biophys. Acta 933*, 22−34.
50. Parson, W. W., Chu, Z. T., and Warshel, A. (1990) *Biochim. Biophys. Acta 1017*, 251−272.
51. Osváth, S., Laczkó, G., Sebban, P., and Maróti, P. (1996) *Photosynth. Res. 47*, 41−49.
52. Fidy, J., Vanderkooi, J. M., Zollfrank, J., and Friedrich, J. (1992) *Biophys. J. 63*, 1605−1612.
53. Trissl, H.-W. (1983) *Proc. Natl. Acad. Sci. U.S.A. 80*, 7173−7177.
54. Drachev, L. A., Semenov, A. Y., Skulachev, V. P., Smirnova, I. A., Chamorovskii, S. K., Kononenko, A. A., Rubin, A. B., and Uspenskaya, N. Y. (1981) *Eur. J. Biochem. 117*, 483−489.
55. Drachev, S. T., Drachev, L. A., Konstantinov, A. A., Semenov, A. Y., Skulachev, V. P., Arutjunjan, A. M., Shuvalov, V. A., and Zaberezhnaya, S. M. (1988) *Eur. J. Biochem. 171*, 253−264.
56. Bibikov, S. I., Bloch, D. A., Cherepanov, D. A., Oesterhelt, D., and Semenov, A. Y. (1994) *FEBS Lett. 341*, 10−14.
57. Lancaster, C. R. D., and Michel, H. (1997) *Structure 5*, 1339−1359.
58. Grant, E. H., Shephard, R. J., and South, G. P. (1978) *Dielectric Behaviour of Biological Molecules in Solution*, Clarendon Press, Oxford.
59. Treutlein, H., Schulten, K., Brünger, A. T., Karplus, M., Deisenhofer, J., and Michel, H. (1992) *Proc. Natl. Acad. Sci. U.S.A. 89*, 75−79.
60. Deisenhofer, J., Epp, O., Huber, R., and Michel, H. (1984) *J. Mol. Biol. 180*, 385−398.

BI001885U